Nitric oxide reactivity accounts for N-nitroso-ciprofloxacin formation under nitrate-reducing conditions

Monica Brienza, Rayana Manasfi, Andrés Sauvêtre, Serge Chiron

Nitric oxide reactivity accounts for N-nitroso-ciprofloxacin formation under nitrate-reducing conditions

Monica Brienza, Rayana Manasfi, Andrés Sauvêtre, Serge Chiron*

UMR HydroSciences Montpellier, Montpellier University, IRD, 15 Ave Charles Flahault 34093 Montpellier cedex 5, France.

*Corresponding author: Tel: + 33 - 411759415; Fax: + 33 - 411759414; e-mail address: serge.chiron@umontpellier.fr

Abstract

The formation of N-nitroso-ciprofloxacin (CIP) was investigated both in wastewater treatment plants including nitrification/denitrification stages and in sludge slurry experiments under denitrifying conditions. The analysis of biological wastewater treatment plant effluents by Kendrick mass defect analysis and liquid chromatography - high resolution - mass spectrometry (LC-HRMS) revealed the occurrence of N-nitroso-CIP and N-nitroso-hydrochlorothiazide at concentration levels of 34 ± 3 ng/L and 71 ± 6 ng/L, respectively. In laboratory experiments and dark conditions, produced N-nitroso-CIP concentrations reached a plateau during the course of biodegradation experiments. A mass balance was achieved after identification and quantification of several transformation products by LC-HRMS. N-nitroso-CIP 14.3 % of the initial CIP concentration (20 µg/L) and accumulated against time. The use of 4,5-diaminofluorescein diacetate and superoxide dismutase as scavengers for *in situ* production of nitric oxide and superoxide radical anion respectively, revealed that the mechanisms of formation of N-nitroso-CIP likely involved a nitrosation pathway through the formation of peroxynitrite and another one through codenitrification processes, even though the former one appeared to be prevalent. This work extended the possible sources of N-nitrosamines by including a formation pathway relying on nitric oxide reactivity with secondary amines under activated sludge treatment.

Keywords: N-nitrosamine; N-nitroso-ciprofloxacin; nitric oxide; activated sludge; biodegradation.

1. Introduction

N-nitrosamines have been ubiquitously detected in different environmental compartments including surface and ground waters (Ma et al., 2012), sludge (Venkatesan et al., 2014), river sediment (Gushgari et al., 2017) and soil (Chiron et al., 2016). Moreover, N-nitroso-dimethylamine (NDMA) has been the most frequently detected N-nitrosamine in drinking water (Russell et al., 2012). Research on N-nitrosamines has been mainly limited to those compounds included in the US EPA Contaminant Candidate List 3, namely N-nitroso-diethylamine (NDEA), NDMA, N-nitroso-di-n-propylamine (NDPA), N-nitroso-diphenylamine (NDPhA), N-nitroso-pyrrolidine (NPYR). However, all secondary and tertiary amines can theoretically undergo nitrosation reactions and there is no clear rationale for only targeting those particular compounds. For instance, N-nitroso-diethanolamine has been found to be a significant component of total N-nitrosamines in recycled wastewater due to the widespread usage of triethanolamine in consumer products (Dai et al., 2015). N-nitroso-morpholine has been detected as a major N-nitrosamine in potable reuse systems (Glover et al., 2019). There is still on-going discussion on sources of N-nitrosamines. These latter have been found to be unintentionally formed during industrial processes such as rubber manufacturing and processing (Beita-Sandi et al., 2019), textile printing and dyeing (Chen et al., 2019) accounting for their frequent detection in industrial wastewaters. Disinfection of waters containing secondary and tertiary amines by chlorination and chloramination (Piazzoli et al., 2018) and to a lesser extent by ozonation (Sgroi et al., 2014) can also result in the formation of N-nitrosamines. Finally, domestic wastewater treatment plant (WWTPs) effluents are also believed to be a major source of N-nitrosamines due to their high content in animal and human urines (Krauss et al., 2009). However, the environmental formation of N-nitrosamines is also a plausible source, which has probably been overlooked up till now. There are now several pieces of observations available in the literature calling for more research in this area. Bacterial nitrosation of secondary amines are common in the environment with for instance, the formation of N-nitroso-ciprofloxacin (CIP) in mixed denitrifying cultures under anoxic conditions (Liu et al., 2013). This reaction has been generally attributed to nitrate reductase or cytochrome cd_1-nitrite reductase

59 through the production of nitric oxide (NO) or NO^+-like species (Calmels et al., 1996) and can be also
60 performed by environmental mycobacteria (Adjei et al., 2006). More recently, the detection of N-
61 nitroso-dibutylamine (NDBA), NDPhA and NPYR in freshwater sediments collected downstream of
62 domestic WWTPs has been rather ascribed to *in situ* formation than to sorption processes. The
63 hydrophilic properties of targeted N-nitrosamines, particularly NPYR with a log k_{ow} = - 0.19 (Gushgari
64 et al., 2017) excluded adsorption to sediment as the main sink for these chemicals. Understanding
65 the mechanisms of N-nitrosamines formation is essential due to the carcinogenic nature of these
66 contaminants. In this context, NO reactivity was considered as a potential pathway for the formation
67 of N-nitrosamines in this work. $NO^{\bullet}$ is a free radical specie and as such a very reactive specie
68 (Heinrich et al., 2013). $NO^{\cdot}$ can be produced by three main chemical and biochemical pathways
69 including 1) heterotrophic denitrification in which nitrite is reduced to $NO^{\cdot}$ by copper- or
70 cytochrome- containing nitrite reductases and autotrophic nitrification processes in which $NO^{\cdot}$ is
71 generated as a by-product, 2) anaerobic ammonium oxidation (anammox) in which $NO^{\cdot}$ is produced
72 as a by-product from nitrite reduction and hydroxylamine oxidation (Rathnayake et al., 2018) and 3)
73 abiotic denitritation in presence of iron(II) (Pilekaard, 2013). Once (bio)generated, $NO^{\cdot}$ can react with
74 (bio)generated superoxide radical anion ($O_2^{\cdot-}$) at diffusion-controlled rate leading to peroxynitrite
75 ($ONOO^-$) which is a strong nitrosating agent responsible for N-nitrosation reactions (Heinrich et al.,
76 2013). Codenitrification is also known to be an N-nitrosation process (Spott et al., 2011).
77 Codenitrification is a microbial pathway, which relies on nitrite and $NO^{\cdot}$ reductases, which are
78 enzymes able to supply an enzymebound nitrosyl compound able to attack nucleophiles such as
79 secondary amines to give N-nitrosamines. Consequently, the main aims of this work were the
80 followings: 1) To investigate the relevance of N-nitrosation reaction in biological wastewater
81 treatment plants (WWTPs) including nitrogen treatment (nitrification and denitrification), 2) to
82 investigate the relevance of N-nitrosation reactions in sludge under nitrate-reducing conditions
83 taking 1-phenylpyperazine and CIP as probe compounds and 3) To discriminate between microbially

mediated N-nitrosation reactions (codenitrification) and abiotic N-nitrosation reactions through peroxynitrite formation.

2. Material and methods

2.1 Chemicals and reagents

Sodium nitrite ($NaNO_2$), sodium azide (NaN_3), 4,5-diaminofluorescein diacetate solution (DAF-2 DA), ciprofloxacin (CIP, > 98%), 1-phenylpiperazine (> 98%), metoprolol (MET, > 98%), hydrochlorothiazide (HCT, > 98%), superoxide dismutase (SOD) from *Escherichia Coli* were obtained from Sigma Aldrich (St Quentin-Fallavier, France). CIP-d_8 (> 98%), desethylene-CIP hydrochloride, N-formyl-CIP (> 98%), 1-nitroso-4-phenylpiperazine (> 97%), HCT-d_2, MET-d_7 hydrochloride were obtained from Toronto Research Chemicals (Toronto, Canada). 4,5-Diaminofluorescein-2 (DAF-2) and triazolofluorescein (DAF-2T) from Santa Cruz Biotechnology (Heidelberg, Germany). Acetonitrile (HPLC grade) was obtained from Carlo Erba (Val de Reuil, France). All solutions were prepared with ultrapure water obtained from a Milli-Q Plus system (Millipore, Bedford, MA). The synthesis of N-nitroso-CIP is reported in Supporting Material (SM).

2.2 Batch biodegradation experiments

A set of anoxic sludge slurries degradation experiments in serum bottles, which were spiked with probe secondary amines at 20 µg/L concentration was conducted as described previously (Brienza et al., 2017) with some modifications. Serum bottles were filled with 150 mL of an effluent collected at a biological wastewater treatment plant (WWTP) and were charged with 1 g of sludge from the WWTP denitrifying tank. Those experiments were carried out in the dark by wrapping serum bottles with aluminum foils because N-nitrosamines are known to be labile compounds in the presence of light (Brienza et al., 2019). To stimulate denitrification processes, nitrate ions at high concentration (50 mg/L) and acetate (1 g/L) as an easily biodegradable organic carbon source, were added to the bottles. The addition of acetate as an exogenous electron donor was necessary since CIP removal was probably driven by heterotrophic bacteria (Liao et al., 2016). Denitrification was clearly indicated by nitrite and nitrate measurements. Oxygen concentration was maintained below 1 mg/L by purging

with N_2 gas for 30 min. Serum bottles were sealed with butyl rubber stoppers and aluminum caps in which syringes were inserted for sample collection. All microcosms were kept at 20 ± 5°C and agitated with magnetic stirrers throughout the whole experiments. Prior to spiking probe compounds (i.e. CIP and 1-phenylpiperazine), the test systems were pre-conditioned for two days. Control experiments void of biological activity were implemented by adding 1 g/L of NaN_3 and aerating the slurries. In this way, aerobic and anoxic respiration were both inhibited by NaN_3 and dissolved oxygen, respectively (Su et al., 2015). At regular time intervals, 1.5 mL of sample were collected, immediately filtered (0.22 µm nylon filter) for nitrate and nitrite analysis. Ten mL were extracted by solid-phase extraction (SPE) following the same protocol as the one applied for WWTPs effluents (see section 2.3). SPE extracts were stored at - 20°C and wrapped in aluminum foil to avoid N-nitrosamines degradation before instrumental analysis. All experiments were carried out in duplicate and results are presented as an average of two experiments.

2.3 Monitoring of selected N-nitrosamines in urban WWTPs effluents

Effluents were collected from two domestic WWTPs located in France namely WWTP1 (20,000 m^3/d), and WWTP2 (34,000 m^3/d). The treatment of WWTP1 and WWTP2 consisted of preliminary treatment, primary sedimentation unit and secondary treatment with biological nutrient removal including nitrogen and phosphorus removal steps. WWTP1 was equipped with a membrane bioreactor (MBR) technology. 24 h composite samples were collected in amber glass bottles. Five hundred mL samples were filtered on 0.45 µm cellulose filter, spiked with 100 ng deuterated CIP, MET and HCT and extracted by SPE using Oasis HLB cartridges (6 mL, 200 mg, Waters Corporation, Milford, MA) within 24 h after collection. Subsequently, the cartridges were dried by purging with nitrogen for 1 h. Prior to analysis, analytes were eluted with 2 x 4 mL of acetonitrile containing 1% acetic acid (v:v). Extracts were then evaporated to dryness with a gentle N_2 gas stream and reconstituted in 500 µL acetonitrile.

2.4 Photolysis experiments.

Distilled water solutions of N-nitroso-CIP (10 mg/L) were irradiated by using a COFOMEGRA Solarbox photo-simulator (Milano, Italy) equipped with a 1.5 kW Xenon arc lamp which was fitted with glass filters to block the transmission of wavelength below λ = 290 nm in order to simulate natural sunlight. Direct photolysis tests in distilled water were performed at 765 W/m^2 and T = 30°C by using a recirculating water cooling system. One mL samples were collected at different time and directly injected in liquid chromatography (LC) - fluorescence detection (FD) and liquid chromatography - high resolution - mass spectrometry (LC-HRMS) for kinetic studies and transformation products (TPs) identification, respectively.

2.5 Analytical methods.

Nitrate and nitrite were determined by conventional spectrophotometric techniques (see SM for details). $NO^{\cdot}$ formation was scavenged by using DAF-2 DA as a chemical trap. DAF-2 DA is a cell-membrane permeable compound that is hydrolyzed intracellularly to give DAF-2. DAF-2 specifically reacts with $NO^{\cdot}$ or $NO^{\cdot}$ derivatives such as dinitrogen trioxide (N_2O_3) or $ONOO^-$ to give the highly fluorescent DAF-2T, which was analyzed by using LC-FD with $\lambda_{excitation}$ = 495 nm and $\lambda_{emission}$ = 515 nm to increase method selectivity (see SM for more details and Fig. 2 SM for reactions and a typical LC-FD chromatogram). For degradation kinetic studies, concentrations of CIP and N-nitroso-CIP were followed in LC-FD using $\lambda_{excitation}$ at 280 nm and $\lambda_{emission}$ at 450 nm. Analyses were performed using a Phenomenex Luna Omega C-18 column (150 x 3 mm i.d., 5 µm particle size) with a flow rate of 0.5 mL/min and an injection volume of 10 µL. A gradient elution mode was applied from 5% A (acetonitrile) / 95% B (water + 0.1% formic acid) to 95% A / 5% B in 25 min and back to the initial conditions in 3 min. LODs were found to be 5 and 2 µg/L for CIP and N-nitroso-CIP, respectively.

SPE extracts from biodegradation experiments and WWTPs effluents were analyzed by LC-HRMS composed of a Dionex Ultimate 3000 liquid chromatograph, equipped with an electrospray source and a Q-Exactive Orbitrap mass spectrometer (Thermo Fisher Scientific, Les Ulis, France) in full scan MS and in MS/MS mode (for more details, see SM).

160 The formation of potential N-nitroso derivatives of pharmaceuticals was investigated by using a
161 Kendrick mass defect analysis for $NO^{\cdot}$ homologues assuming that the formation of mononitrosated
162 compounds was usually the rule. In a first phase, a deconvolution of the TIC of samples was
163 performed. In a second phase, the measured accurate masses of precursors and TPs were converted
164 to Kendrick masses (KM) with [NO - H] as reference moiety (Eq. 1) and the respective Kendrick mass
165 defect (KMD) was calculated (Eq. 2). Then, precursors and their nitrosated derivatives were
166 distinguished among all pairs of precursors / TPs because their Kendrick mass (KM_{TP}) was shifted by a
167 multiple of 29 (Eq. 3) while their Kendrick mass defect (KMD_{TP}) remained the same with a precision of
168 2 mDa (Eq. 4), as previously recommended (Merel et al., 2017).

169 KM = measured accurate mass x 29 / 28.99016 (1)

170 KMD = KM - nominal KM (2)

171 $KM_{TP} = 29 + KM_{precursor}$ (3)

172 $KMD_{TP} = KMD_{precursor} \pm 2$ mDa (4)

173

174 ## 3. Results and discussion

175 ### 3.1 Field observations

176 Effluents from two biological WWTPs including nitrification and denitrification stages were analyzed
177 in an attempt to investigate the occurrence of N-nitrosation reactions in activated sludge treatment.
178 A suspect screening workflow by using a list of secondary amine pharmaceuticals with their
179 respective exact masses was established on the basis of the knowledge of pharmaceuticals which are
180 able to generate N-nitrosamines in presence of nitrite ions at acidic pH (Brambilla et al., 2007). This
181 approach allowed for the detection and quantification of some pharmaceuticals among which CIP,
182 the β-blocker metoprolol (MET) in the positive ionization mode and the diuretic agent
183 hydrochlorothiazide (HCT) in the negative ionization mode. Their identification was based on

matches with authentic standards. Quantification was carried out by spiking deuterated isotopes of CIP, MET and HCT and by determining recoveries of those compounds (between 70 and 100%) in real wastewater samples. Concentrations of 312 ± 25 and 445 ± 36 ng/L (CIP), 245 ± 29 and 296 ± 36 ng/L (MET), 632 ± 57 and 886 ± 80 ng/L (HCT) were found in WWTP1 and WWTP2 effluents, respectively. Kendrick mass defect analysis for $NO^{\cdot}$ homologues allowed for the identification of N-nitroso-CIP and N-nitroso-HCT, while N-nitroso-MET was never detected. Fig. 1a and 1b show typical Extracted Ion Chromatograms (EICs) corresponding to the analysis of WWTP2 effluent in positive and negative mode of ionization, respectively. HCT has three potential sites for N-nitrosation but only the 4-nitroso derivative was suggested to be formed due to the ready nitrosation of aromatic amines (Gold and Mirvish, 1977). Inserts in Fig. 1a and Fig. 1b show the Kendrick mass plots for CIP and HCT and their respective N-nitroso derivatives with consistent KMD values below 2 mDa. Finally, as a rule of thumb, N-nitroso derivatives exhibited higher retention times than their respective precursors using a C-18 LC column. This behavior was used as an additional piece of evidence for the identification of N-nitroso compounds. The concentration of N-nitroso-CIP was determined to be 34 ± 3 ng/L while that of N-nitroso-HCT was estimated at 71 ± 6 ng/L by using HCT-d_2 as an internal standard. The amount of formed N-nitroso compounds depended on nitrosation rate but also on the stability of N-nitroso compounds in water. Piperazine, N-methylaniline are rapidly nitrosated amines while dialkyl are slowly nitrosated due to the strong basicity of the amine. Nitrosation increased as the basicity of the amine decreased (HCT (pKa 7.9) > CIP (pKa 8.7) > MET (pKa > 9.7), probably accounting for the lack of detection of N-nitroso-MET. Identified N-nitroso compounds were more hydrophobic than that their precursors due to higher retention times in C-18 column. Higher bioavailability was consequently expected in comparison to their parent compounds. N-nitroso-HCT and N-nitroso-CIP could represent a hazard only if they were stable. However, their stability in receiving waters was not easy to predict. Consequently, lab-scale experiments were carried out to account for the formation of N-nitroso compounds formation under denitrifying conditions by using CIP and 1-phenylpiperazine as probe compounds (see section 3.2).

3.2 Batch biodegradation experiments

N-nitrosamines are known to be more stable under biodegradation than under photolysis. To investigate the formation of N-nitroso-CIP, sludge slurry batch experiments spiked with 20 µg/L CIP or 1-phenylpiperazine were conducted under anoxic conditions, allowing for denitrification to proceed. Denitrification was clearly indicated by the decrease in nitrate concentrations and the increase in nitrite concentrations (Fig. 2a). First, biotransformation pathways were investigated by identifying TPs following a suspect screening workflow in LC-HRMS. For this purpose, a database was made up of a list of possible TPs with their molecular formula, exact mass and structure (see Table 1SM). This list was established from a literature search of TPs of CIP formed during photochemical experiments, other oxidative treatments and biodegradation/metabolism experiments. In a first step, TPs with intensities lower than 1 $x10^4$ cps, signal to noise ratios lower than 10, isotopic ratios higher than 10%, and mass accuracy errors higher than 5 mg/L were eliminated. When possible, after preliminary identification based on specific accurate mass (m/z), the potential TPs were further confirmed by including the screening of known fragments ions and the MS/MS spectrum information was compared with that reported in previous literature reports. Following this approach, four TPs were detected including desethylene-CIP, N-formyl-CIP, N-acetyl-CIP and N-nitroso-CIP after the deconvolution of the TIC of samples (see Fig. 3SM for a typical EIC). A peak with a lower area after biological treatment was assigned to a parent compound, while peaks with a higher area were considered as TPs. Desethylene-CIP, N-formyl-CIP and N-nitroso-CIP were confirmed by using authentic standards while N-acetyl-CIP was confirmed by comparing its MS/MS profile with that available in the literature (Liu et al., 2013). Consequently, the biotransformation of CIP involved both the addition of formyl, acetyl and nitroso groups on secondary amines and the oxidation and breakdown of the piperazine ring (see Fig. 3). 1-phenylpiperazine followed the same biotransformation pathways as CIP (see Fig. 4SM for an EIC and Fig 5SM for a proposed transformation pathway). Desethylene CIP might originate from the further transformation of N-nitroso-CIP. Indeed, α-hydroxylation of alkyl N-nitrosamines, which are catalyzed by a variety of

236 oxidases and oxygenases such as cytochrome P450 enzymes has been established (Mesic et al.,
237 2000). The resulting hydroxy-N-nitroso compounds are not stable and further decompose following a
238 dealkylation reaction which might account for the formation of desethylene-CIP.
239 In the time series experiments (Fig. 2b), CIP was hardly degraded (less than 5% of the initial CIP
240 concentration) in control experiments in which the biological activity was inhibited (results not
241 shown). In contrast, in non-control experiments, the decrease in CIP concentration was correlated
242 positively to the increase in identified TPs concentrations. While the concentrations of N-nitroso-CIP,
243 N-acetyl-CIP and N-formyl-CIP stabilized at the end of the experiment time, the concentration of
244 desethylene-CIP dropped likely due to a quicker further transformation of this compound. CIP
245 showed a pronounced bi-phasic degradation with a faster initial phase followed by a slower decline
246 after 90 min incubation time. The CIP degradation slowdown was concomitant to that of nitrate and
247 denitrification was not completed at the end of experiments (8 d). This specific kinetic profile was
248 ascribed to the partial reversibility of N-nitrosation reactions associated with CIP formation. The
249 assumption of TPs toxicity for bacteria was discarded because conjugation reactions are thought to
250 be used by bacteria to reduce the fluoroquinolone antibiotic toxicity (Prieto et al.,2011). CIP TPs were
251 available as standards so that their quantification was possible. A mass balance could be determined
252 during biodegradation experiments and was mostly achieved (Fig. 2b). This result was related to the
253 high dilution rate of sludge (1 g/L) in biodegradation experiments, avoiding nearly all sorption
254 processes of CIP and of its TPs (Polezel et al., 2015). At 96 min of incubation, the concentrations of N-
255 formyl-CIP, N-acetyl-CIP, N-nitroso-CIP and desethylene-CIP were 5.24, 4.38, 3.06 and 1.93 µg/L
256 respectively, accounting for 31.1, 23.2, 14.3, 8.7% of the initial CIP concentration (20 µg/L),
257 respectively. N-formylation reaction was always predominant over the other transformation
258 reactions. The introduction of DAF-2 DA (5 µM) in the biological reactor after 60 min incubation, as a
259 $NO^{\cdot}$ scavenger, fully inhibited the production of N-nitroso-CIP (Fig. 2c) but did not affect the
260 formation of other TPs. This result indicated that the formation of N-nitroso-CIP was directly related
261 to the *in situ* production of $NO^{\cdot}$ through microbial activities. The lack of N-nitrosation reaction well-

correlated to the ending in decrease of CIP biodegradation. Experiments with superoxide dismutase (SOD) were carried out in an attempt to distinguish the contribution of N-nitrosation processes through codenitrification and N-nitrosation reactions through the production of peroxynitrite, because superoxide dismutase is a well-known $O_2^{\cdot-}$ scavenger. The production of this latter was required for the formation of peroxynitrite. The formation of N-nitroso-CIP was only partially inhibited in the presence of SOD (Fig. 2d). The inhibition percentage of N-nitroso-CIP formation ranged from 60.5 to 77.7% depending on the sampling time. Consequently, both N-nitrosation processes (codenitrification and nitrosation through peroxynitrite formation) were operating in the biodegradation system but the peroxynitrite pathway predominated. The pH dependence of N-nitroso-CIP and 1-nitroso-4-phenylpiperazine generation was also investigated. Fig. 4a shows the production of these two N-nitroso compounds against pH. When pH was increased from 4.5 to 6.5, the concentration of these N-nitroso compounds decreased, while their concentrations stabilized after pH 6.5. This experimental result demonstrated a high contribution of nitrous acid (HNO_2) to the formation of N-nitrosamine at pH below 6.5 due to a pKa (HNO_2/NO_2^-) value of 3.4. The contribution of HNO_2 became minimum at pH higher than 6.5. Fig. 4b shows the dependence of N-nitroso-CIP and 1-nitroso-4-phenylpiperazine generation on the concentration of hydrogenocarbonate ions (HCO_3^-). Their concentrations decreased when the concentration of HCO_3^- increased. This result was likely due to the formation of a carbamate adduct resulting from the interaction of secondary amines with CO_2/HCO_3^- (Sun et al., 2011). These carbamate adducts inhibited the nitrosation reactions with HCO_3^- concentration values below 450 mg/L, which are common values in domestic wastewaters. After a threshold value of 450 mg/L, HCO_3^- had a very limited impact on N-nitroso compounds formation.

3.3 Stability of N-nitroso-ciprofloxacin

Even though N-nitroso-CIP was found to be rather stable under biodegradation in our experimental conditions, abiotic transformations might be responsible for its disappearance under real environmental conditions. Denitrosation reactions of N-nitrosamines in water have been reported and have been found to be acid-catalyzed via the formation of N-protonated intermediates

(Sidgwick, 1966). However, in 0.1 M phosphate buffer (pH = 7.5), N-nitroso-CIP was found to be stable for at least 8 d at 25 °C (results not shown). In contrast, N-nitroso-CIP underwent fast decomposition under simulated solar light irradiation through direct photolysis (see insert Fig. 5). Direct photolysis of N-nitroso-CIP was found to follow a first-order kinetic model ($R^2 > 0.99$) with a kinetic constant value of $k = 0.0225 \pm 1.5 \times 10^{-3}$ min^{-1} corresponding to a half-life of 30.8 ± 1.8 min (see insert of Fig. 5). This half-life value was almost twice longer than that of NDMA under identical conditions (i.e., irradiations of 765 W/m^2, (Plumlee and Reinhard, 2007)). Photo-TPs were also identified by LC-HRMS using the suspect screening workflow implemented for CIP biotransformation experiments. Following this approach, several TPs were identified (see a typical Extracted Ion Chromatogram (EIC) and a proposed transformation pathway in Fig. 5) including CIP, desethylene-CIP and 7-amino-1-cyclopropyl-6-fluoro-4-oxo-1,4-dihydroquinoline-3-carboxylic acid (CIP_{263}). A mass balance was determined throughout the photolysis experiments (see Fig. 6SM) and the reverse reaction of N-nitroso-CIP into CIP was found to be the main transformation pathway, likely through a photohydrolysis mechanism similarly to NDMA decomposition under direct photolysis (Lee et al., 2005a). At the end of the reaction time (150 min), CIP concentration reached a value of 6.92 mg/L (i.e. almost 70% of the initial concentration of N-nitroso-CIP). Dealkylation reactions of N-nitroso-CIP into desethylene-CIP (0.25 mg/L after 150 min reaction time) and dealkylation reactions of desethylene-CIP into 7-amino-1-cyclopropyl-6-fluoro-4-oxo-1,4-dihydroquinoline-3-carboxylic acid (2.25 mg/L after 150 min reaction time) were a minor pathway and consistent with a photooxidation mechanism in presence of oxygen, as previously reported for NDMA (Lee et al., 2005b).

4. Conclusions

This study was carried out to investigate the potential nitrosation reaction of CIP in denitrifying sludge conditions by using the combined results of lab controlled experiments and those from a monitoring survey of the effluents of two domestic biological WWTPs. Lab experiments revealed that

313 N-nitroso-CIP was generated and accumulated against time, accounting for 14.3% of the initial spiked
314 CIP concentration in sludge slurries under anoxic conditions. N-nitroso-CIP formation was found to be
315 due to $NO^{\cdot}$ reactivity, which was generated during denitrification processes. The involvement of $NO^{\cdot}$
316 through $ONOO^{-}$ in the formation of N-nitroso-CIP resulted in a new formation pathway of N-
317 nitrosamines under activated sludge treatment. N-nitroso-CIP underwent much faster direct
318 photolysis than biodegradation, mainly leading back to CIP. Consequently, N-nitroso-CIP might
319 survive in water with low transmittance and in sediment. This assumption was confirmed by the
320 detection of N-nitroso-CIP in cloudy urban WWTPs effluents. The occurrence of N-nitroso-CIP in
321 WWTP effluent was about 10% of initial CIP concentration in influent. The determined concentration
322 of 34 ± 3 ng/L was not expected to be of high toxicity to human beings but N-nitroso-CIP might
323 preserve some biological activity and contribute to the spread of antibiotic-resistant bacteria and
324 genes. This latter point should deserve further investigation, because a recent study observed that
325 the denitrifying bacteria Brachymonas, Candidatus Competibacter, Thiobacillus and Steroidobacter
326 are important antibioticresistant genes hosts (including genes against quinolones) in pig farm anoxic-
327 oxic wastewater treatment processes (Yang et al, 2020) and might participate to CIP
328 biotransformation.
329
330
331 Acknowledgements: This research was financially supported by the Water and Agriculture, Food
332 Security and Climate Change Joint Programming Initiatives (JPIs) through the research project
333 AWARE “Assessing the fate of pesticides and waterborne contaminants in agricultural crops and their
334 environmental risks”.
335
336 References

Adjei, M., Heinze, T., Deck, J., Freeman, J., Williams, A., Sutherlan, J., 2006. Transformation of the antibacterial agent norfloxacin by environmental mycobacteria, Appl. Environ. Microbiol. 72, 5790-5793.

Beita-Sandi, W., Selbes, M., Ersan, M., Karanfil, T., 2019. Release of nitrosamines and nitrosamine precursors from scrap tires, Environ. Sci. Technol. Lett. 6, 251-256.

Brambilla, G., Martelli, A., 2007. Genotoxic and carcinogenic risk to humans of drug-nitrite interaction products, Mutation Res. 635, 17-52.

Brienza, M., Duwig, C., Perez, S., Chiron, S., 2017. 4-Nitroso-sulfamethoxazole generation in soil under denitrifying conditions: Field observations versus laboratory results, J. Hazard. Mater. 334, 185-192.

Brienza, M., Manasfi, R., Chiron, S., 2019. Relevance of N-nitrosation reactions for secondary amines in nitrate-rich wastewater under UV-C treatment, Water Res. 162, 22-29.

Calmels, S., Ohshima, H., Henry, Y., Bartsch, H., 1996. Characterization of bacterial cytochrome cd_1-nitrite reductase as one enzyme responsible for catalysis of nitrosation of secondary amines, Carcinogenesis 17, 533-536.

Chen, W., Chen, Y., Huang, H., Lu, Y., Khorram, M., Zhao, W., Wang, D., Qi, S., Jin, B., Zhang, G., 2019. Occurrence of N-nitrosamines in the Pearl River delta of China: Characterization and evaluation of different sources, Water Res. 164, 114896.

Chiron, S., Duwig, C., 2016. Biotic nitrosation of diclofenac in a soil aquifer system (Katari watershed, Bolivia), Sci. Total Environ. 565, 473-480.

Dai, N., Zeng, T., Mitch, W., 2015. Predicting N-nitrosamines: N-nitrosodiethanolamine as a significant component of total N-nitrosamines in recycled wastewater, Environ. Sci. Technol. Lett. 2, 54-58.

Glover, C., Verdugo, E., Trenholm, R., Dickenson, E., 2019. N-nitrosomorpholine in potable reuse, Water Res. 148, 306-313.

362 Gold, B., Mirvish, S., 1977. N-nitroso derivatives of hydrochlorothiazide, niridazole, and tolbutamide,
363 Toxicol. Appl. Pharmacol. 40, 131-136.
364 Gushgari, A., Halden, R., Venkatesan, A., 2017. Occurrence of N-nitrosamines in U.S. freshwater
365 sediments near wastewater treatment plants, J. Hazard. Mater. 323, 109-115.
366 Heinrich, T., da Silva, R., Miranda, K., Switzer, C., Wink, D., Kukuto, J., 2013. Biological nitric oxide
367 signaling: chemistry and terminology, British J. Pharmacol. 169, 1417-1429.
368 Krauss, M., Longrée, P., Dorush, F., Ort, C., Hollender, J., 2009. Occurrence and removal of N-
369 nitrosamines in wastewater treatment plants, Water Res. 43, 4381-4391.
370 Lee, C., Choi, W., Yoon, J., 2005a. UV photolytic mechanism of N-nitrosodimethylamine in water:
371 Dual pathways to methylamine versus dimethylamine, Environ. Sci. Technol. 39, 2101-2106.
372 Lee, C., Choi, W., Yoon, J., 2005b. UV photolytic mechanism of N-Nitrosodimethylamine in water:
373 Roles of dissolved oxygen and solution pH, Environ. Sci. Technol. 39, 9702-9709.
374 Liao, X., Li, B., Zou, R., Dai; Y. Xie, S., Yuan, B., 2016. Biodegradation of antibiotic ciprofloxacin:
375 pathways, influential factors, and bacterial community structure. Environ. Sci. Pollut. Res. 23,
376 7911-7918.
377 Liu, Z., Sun, P., Palovtathis, S., Zhou, X., Zhang, Y., 2013. Inhibitory effects and biotransformation
378 potential of ciprofloxacin under anoxic/anaerobic conditions, Biores. Technol. 150, 28-35.
379 Ma, F., Wan, Y., Yuan, G., Meng, L., Dong, Z., Hu, J., 2012. Occurrence and source of nitrosamines and
380 secondary amines in groundwater and its adjacent Jialu River basin. China, Environ. Sci.
381 Technol. 46, 4236-4243.
382 Merel, S., Lege, S., Yanes Heras, J., Zwiener, C., 2017. Assessment of N-oxide formation during
383 wastewater ozonation, Environ. Sci. Technol. 51, 410-417.
384 Mesic, M., Peuralahti, J., Blans, P., Fishbein, J., 2000. Mechanisms of decomposition of α-
385 hydroxydialkylnitrosamines in aqueous solution, Chem. Res. Toxicol. 13, 983-992.

386 Piazzoli, A., Breider, F., Gachet-Aquillon, C., Antonelli, M., von Gunten, U., 2018. Specific and total N-
387 nitrosamines formation potentials of nitrogenous micropollutants during chloramination,
388 Water Res. 135, 311-321.
389 Pilekaard, K., 2013. Processes regulating nitric oxide emissions from soils, Phil. Trans. R. Soc. B 368,
390 20130126.
391 Plumlee, M., Reinhard, M., 2007. Photochemical attenuation of N-nitrosodimethylamine (NDMA) and
392 other nitrosamines in surface water, Environ. Sci. Technol. 41, 6170-6176.
393 Polezel, F., Lehnberg, K., Dott, W., Trapp, S., Thomas, K., Plosz, B., 2015. Factors influencing sorption
394 of ciprofloxacin onto activated sludge: Experimental assessment and modelling implications,
395 Chemosphere 119, 105-111.
396 Prieto, A., Möder, M., Rodil, R., Adrian, L., Marco-Urrea, E., 2011. Degradation of the antibiotics
397 norfloxacin and ciprofloxacin by a white-rot fungus and identification of degradation
398 products, Biores. Technol. 102, 10987-10995.
399 Rathnayake, R., Oshiki, M., Ishii, S., Segawa, T., Satoh, H., Okab, S., 2018. Experimental evidence for *in*
400 *situ* nitric oxide production in anaerobic ammonia-oxidizing bacterial granules, Environ. Sci.
401 Technol. 52, 5744-5752.
402 Russell, C., Blute, N., Via, S., Wu, X., Chowdhury, Z., More, R., 2012. Nationwide assessment of
403 nitrosamine occurrence and trends, J. AWWA 104, E205−E217.
404 Sgroi, M., Roccaro, P., Oelker, G., Snyder, S., 2014. N-Nitrosodimethylamine formation upon
405 ozonation and identification of precursors source in a municipal wastewater treatment plant,
406 Environ. Sci. Technol. 48, 10308-10315.
407 Sidgwick, N., 1966. The organic chemistry of nitrogen, 3rd ed., revised by I. T. Millar and H. D.
408 Springall. Clarendon Press, Oxford, United Kingdom p.63.
409 Spott, O., Russow, R., Stange, C., 2011. Formation of hybrid N_2O and hybrid N_2 due to
410 codenitrification: first review of a barely considered process of microbially mediated N-
411 nitrosation, Soil Biol. Biochem. 243, 1995-2011.

412 Su, L., Aga, D., Chandran, K., Khunjar, W., 2015. Factors impacting biotransformation kinetics of trace
413 organic compounds in lab-scale activated sludge systems performing nitrification and
414 denitrification, J. Hazard. Mater. 282, 116-124.
415 Sun, Z., Liu, Y., Zhong, R., 2011. Carbon dioxide in the nitrosation of amine: Catalyst or inhibitor? J.
416 Phys. Chem. A 115, 7753-7764.
417 Venkatesan, A., Pycke, B., Halden, R., 2014. Detection and occurrence of N-nitrosamines in archives
418 biosolids from the targeted national sludge survey of the U.S. Environmental Protection
419 Agency, Environ. Sci. Technol. 48, 5085-5092.
420 Yang, Y., Wu, R., Hu, J., Xing, S., Huang, C., Mi, J., Liao, X., 2020. Dominant denitrifying bacteria are
421 important hosts of antibiotic resistance genes in pig farm anoxic-oxic wastewater treatment
422 processes. Environ. Intern. 143, 105897.

423

Fig. 1. Extracted Ion Chromatograms (EICs) corresponding to the analysis of a WWTP2 effluent sample where (a) CIP, N-nitroso-CIP, (b) HCT and N-nitroso-HCT were detected and precursors and N-nitroso derivatives on Kendrick mass plots (inserts)

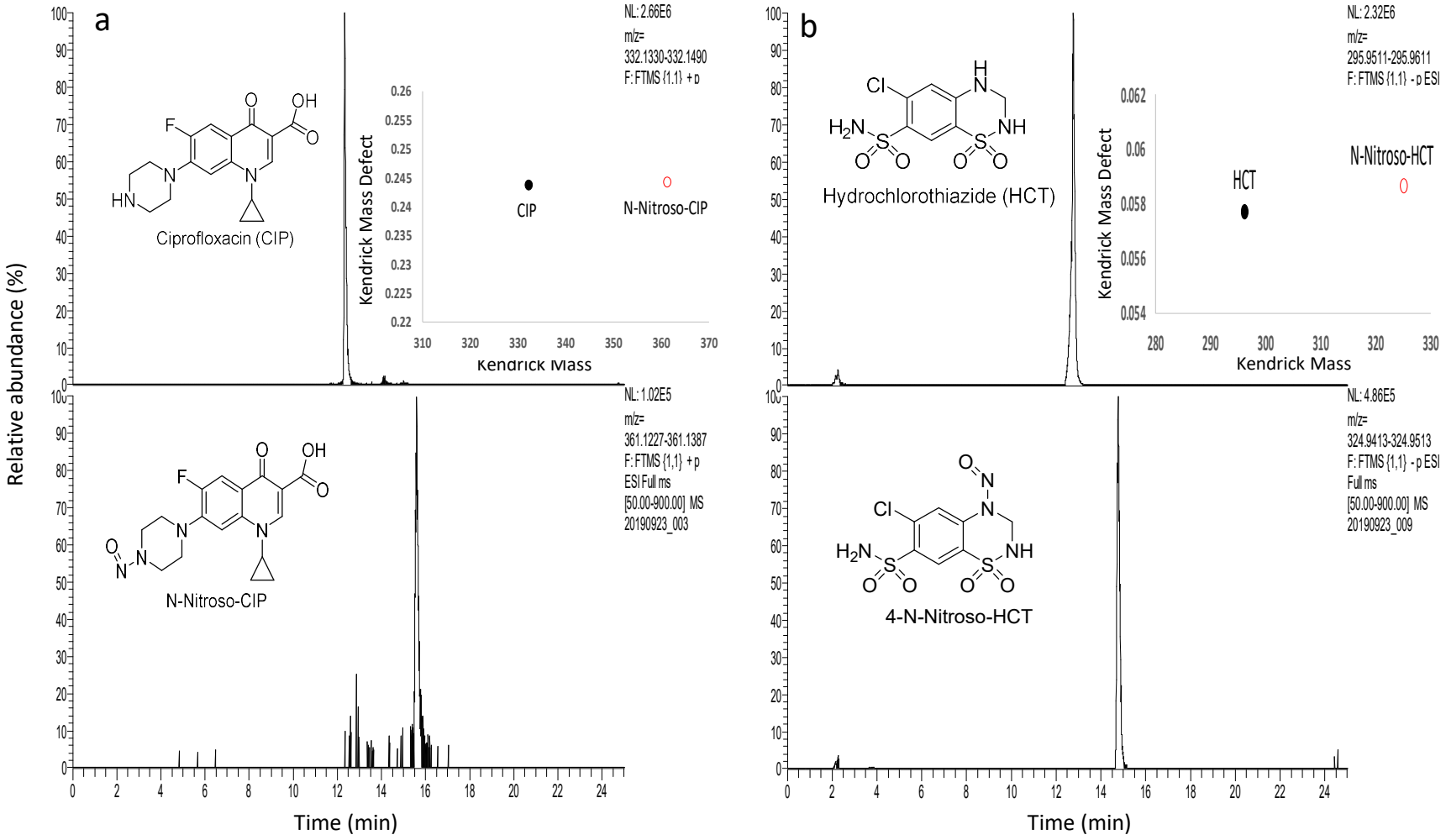

Fig. 2. a) Time evolution of concentrations of nitrate and nitrite ions, b) Time evolution of CIP and its TPs in sludge slurry under denitrifying conditions, c) Time evolution of CIP and its TPs after adding DAF-2 DA as a $NO^{\cdot}$ scavenger, d) Tile evolution of CIP and its TPs after adding superoxide dismutase (SOD) as a superoxide anion radical scavenger. All data were collected during sludge slurry experiments at pH 7.8 and T=25°C. Initial [NO_3^-]=50 mg/L, initial [CIP]=20 µg/L.

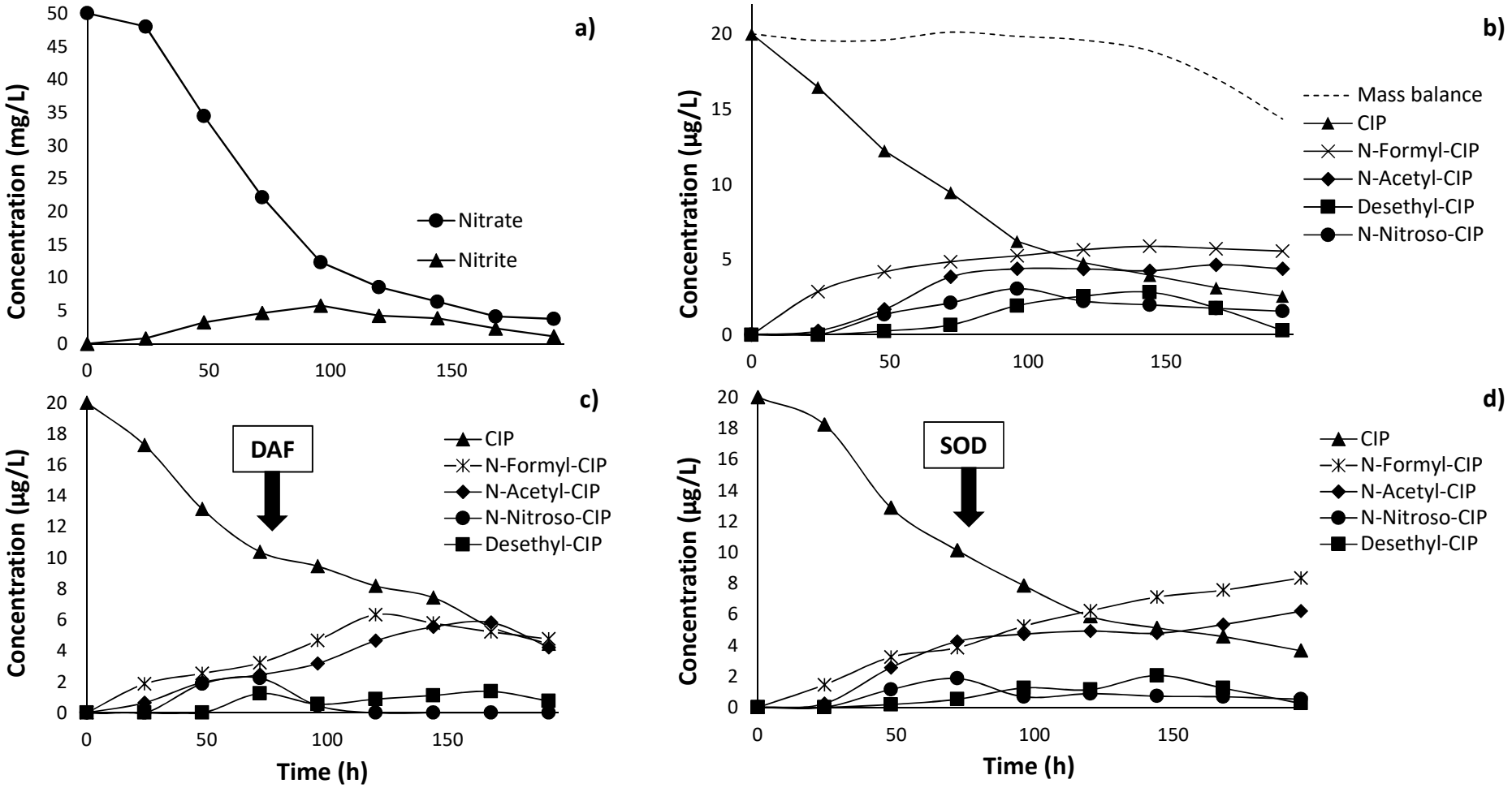

Fig. 3. Proposed transformation pathways of CIP in sludge under denitrifying conditions.

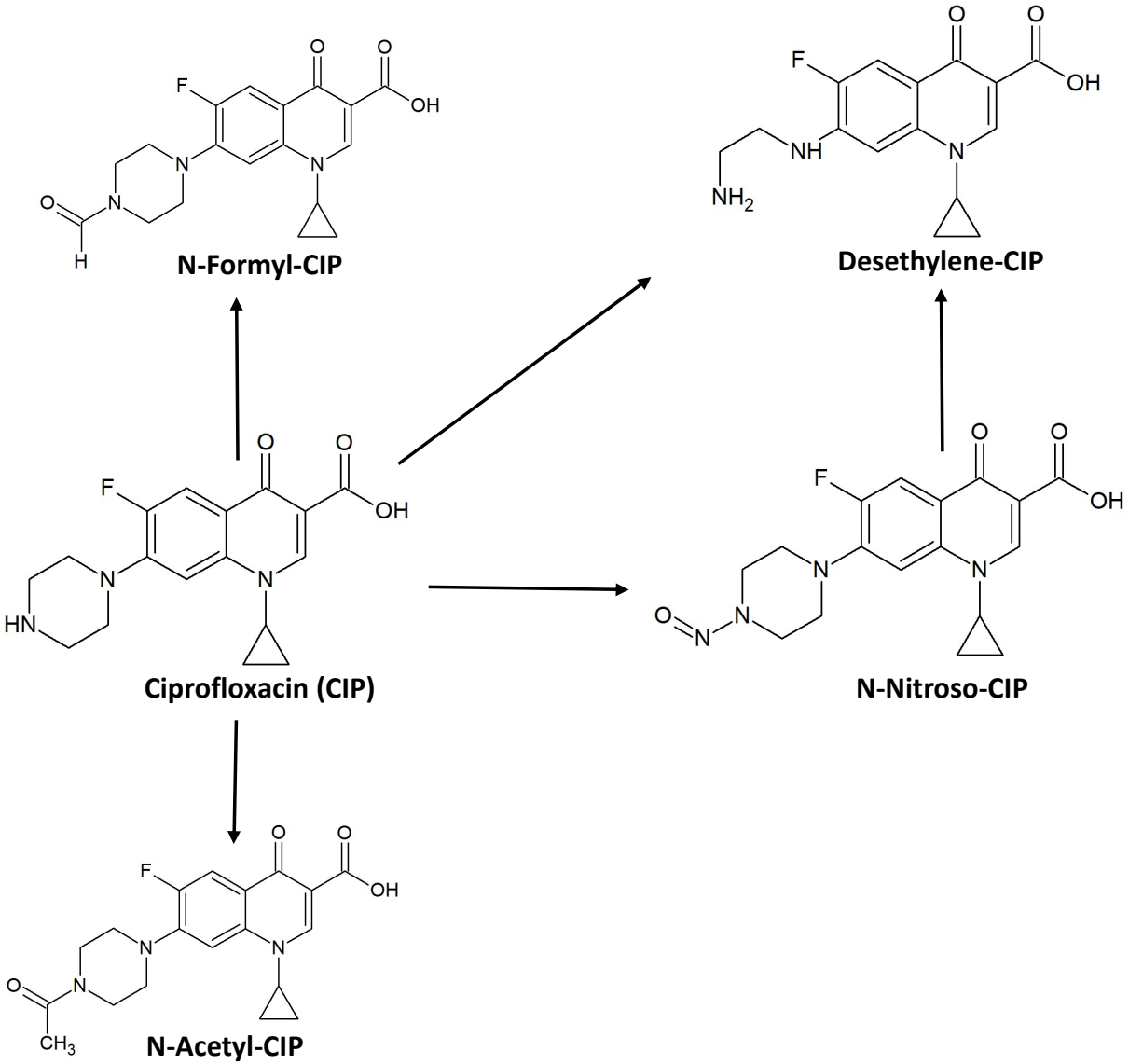

Fig. 4. a) pH and b) [HCO_3^-] concentration effects on the formation of N-nitroso-CIP and 1-nitroso-4-phenylpiperazine

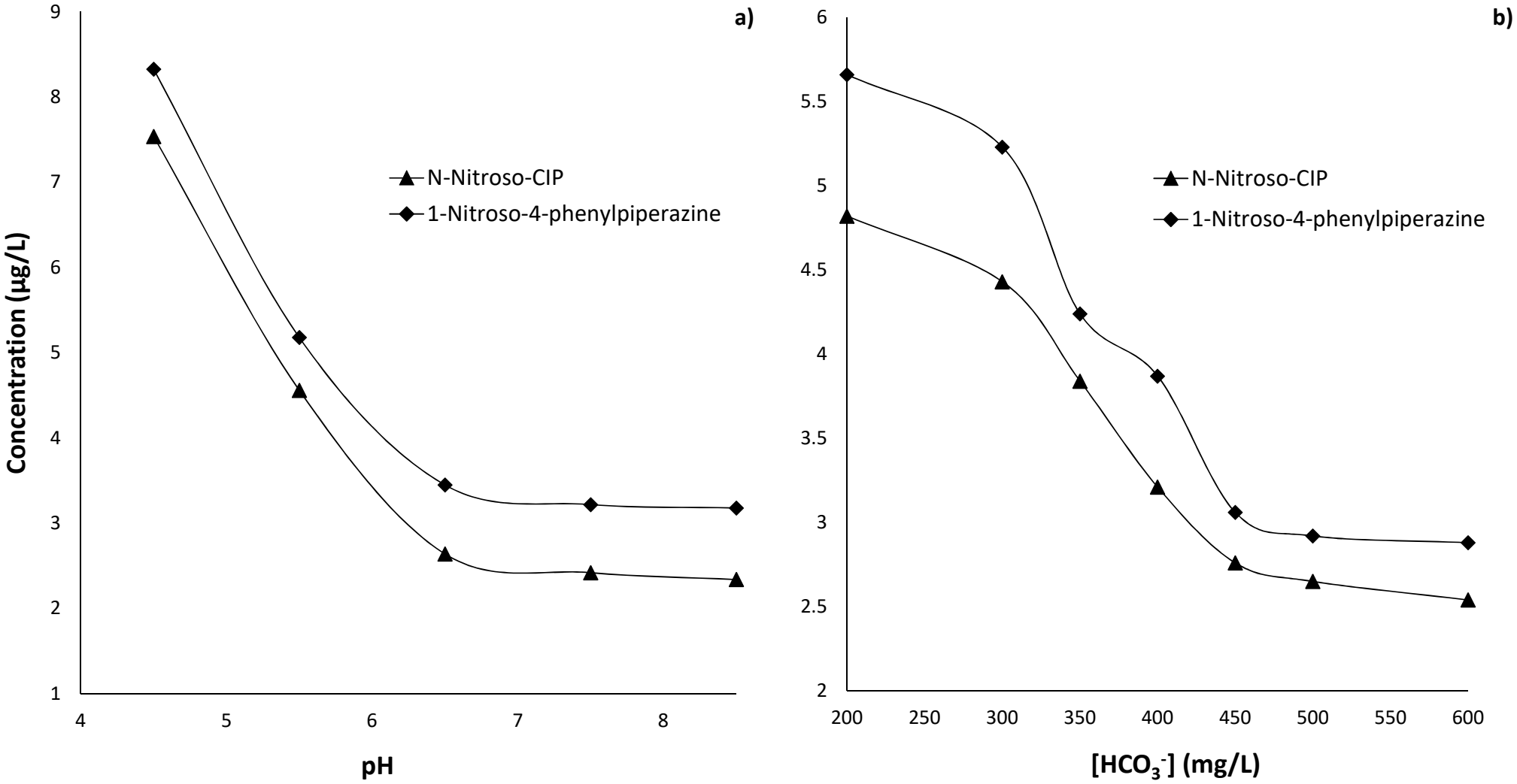

Fig. 5. Extracted Ion Chromatogram (EIC) corresponding to N-nitroso-CIP photolysis. Inserts: a)Proposed transformation pathway and b) First order kinetic plots.

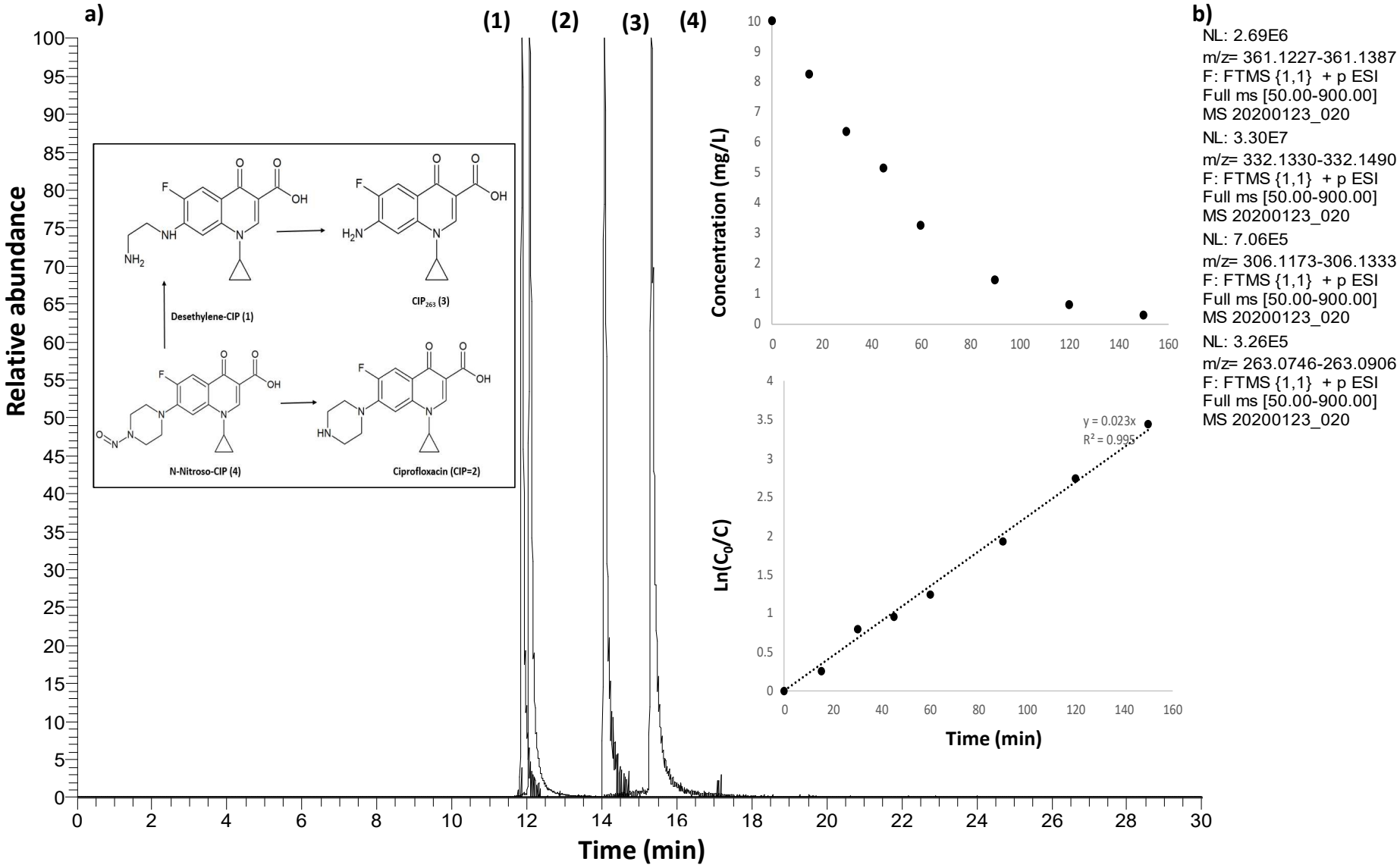

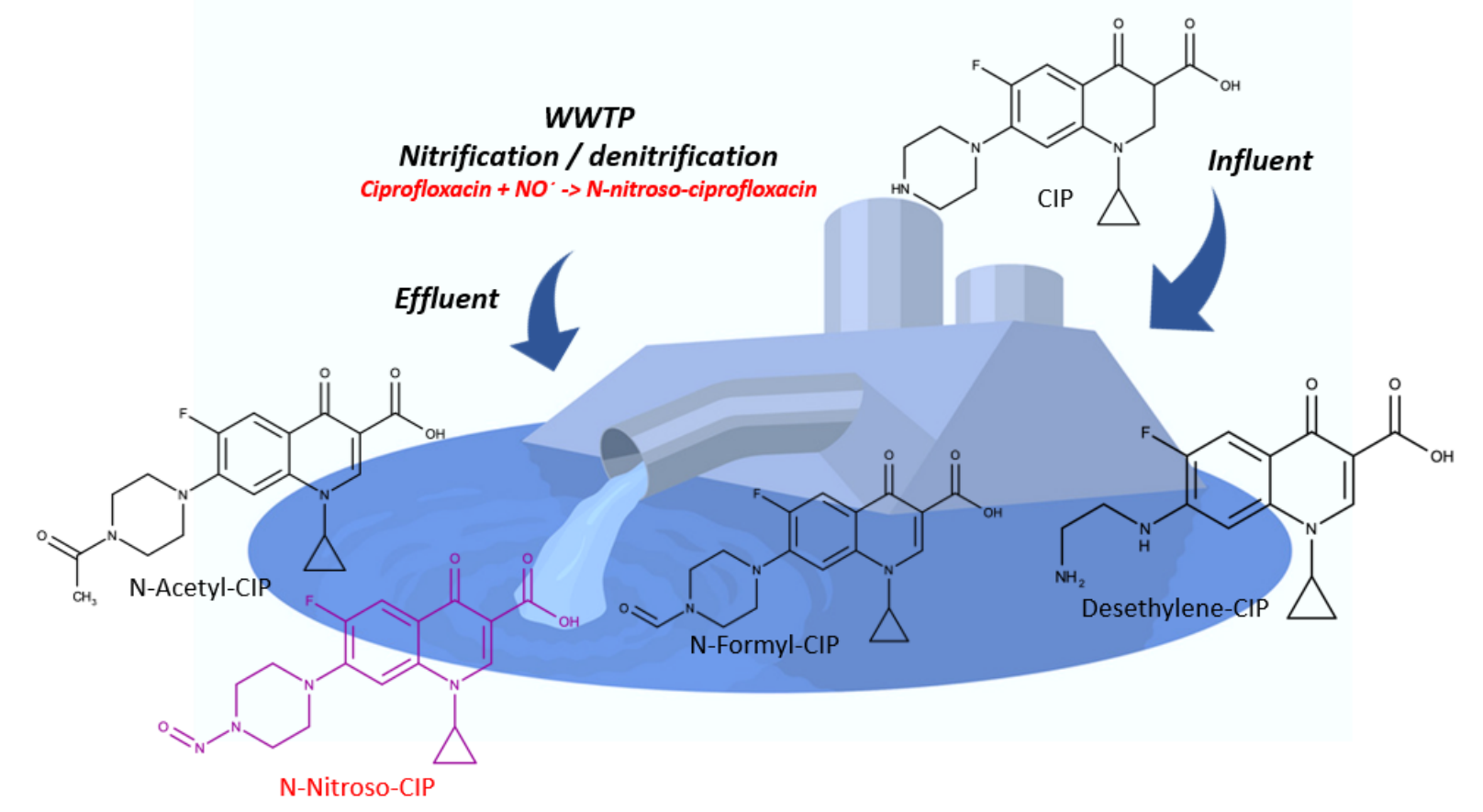
WWTP
Nitrification / denitrification
Ciprofloxacin + NO˙ -> N-nitroso-ciprofloxacin
Influent
Effluent
CIP
N-Acetyl-CIP
N-Formyl-CIP
Desethylene-CIP
N-Nitroso-CIP